Ferromagnetism and superconductivity in artificial crystals

NTT Basic Research Laboratories

Hideaki Takayanagi

Hiroyuki Tamura

***Kenji Shiraishi**

Takashi Kimura

Tatsushi Akazaki

Andreas Richter

**Tsukuba University*

Overview

1. Artificial crystals designed in dot arrays
   - Quantum dot system (Artificial atom, molecule, crystal)
   - Design of Lieb and kagome lattices having flat-band
   - Advantages of using dot arrays for flat-band system
2. Flat-band ferromagnetism in quantum dot arrays
   - Stability of ferromagnetism in dot arrays
   - Kagome lattice designed in quantum wire network
3. Sample structures
4. Superconductivity on a plaquette lattice
5. Summary

Artificial Material using Semiconductor Dots

Single dot

Atomic properties in an “artificial atom”

→ Shell structure, Hund’s rule, and Kondo effect

Coupled dots

Molecular properties in an “artificial molecule”

→ Bonding and anti-bonding level splitting

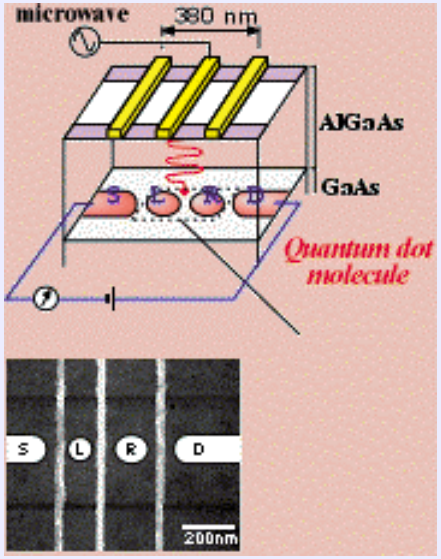

Dot arrays

“Artificial crystals” by treating a dot as a building block

→ Various lattice design

→ Flat-band ferromagnetism

→ Superconductivity

Lattice Structures having Flat-band

Lieb lattice

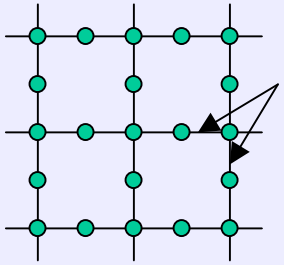

Bipartite lattice

Kagome lattice

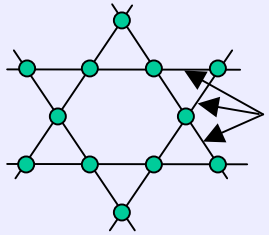

Line graph

Single-particle band diagram

Tight-binding approximation

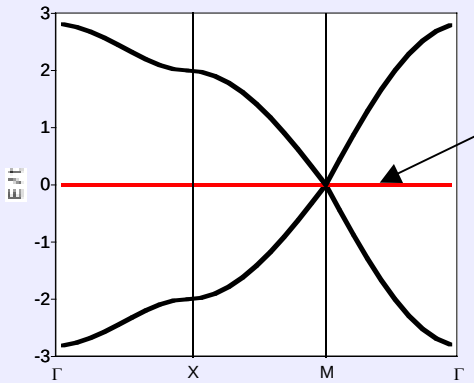

2D Lieb lattice

Flat-band

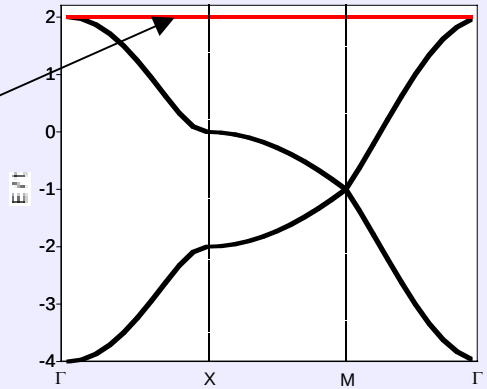

2D kagome lattice

Ferromagnetism appears when the flat band is half-filled.

E. H. Lieb, PRL **62**, 1201 (’89)

A. Mielke, J. Phys A **24,** L63 (’91)

Origin of Word “Kagome”

kago-me

kago（籠）= basket

me（目）= mesh (or pattern)

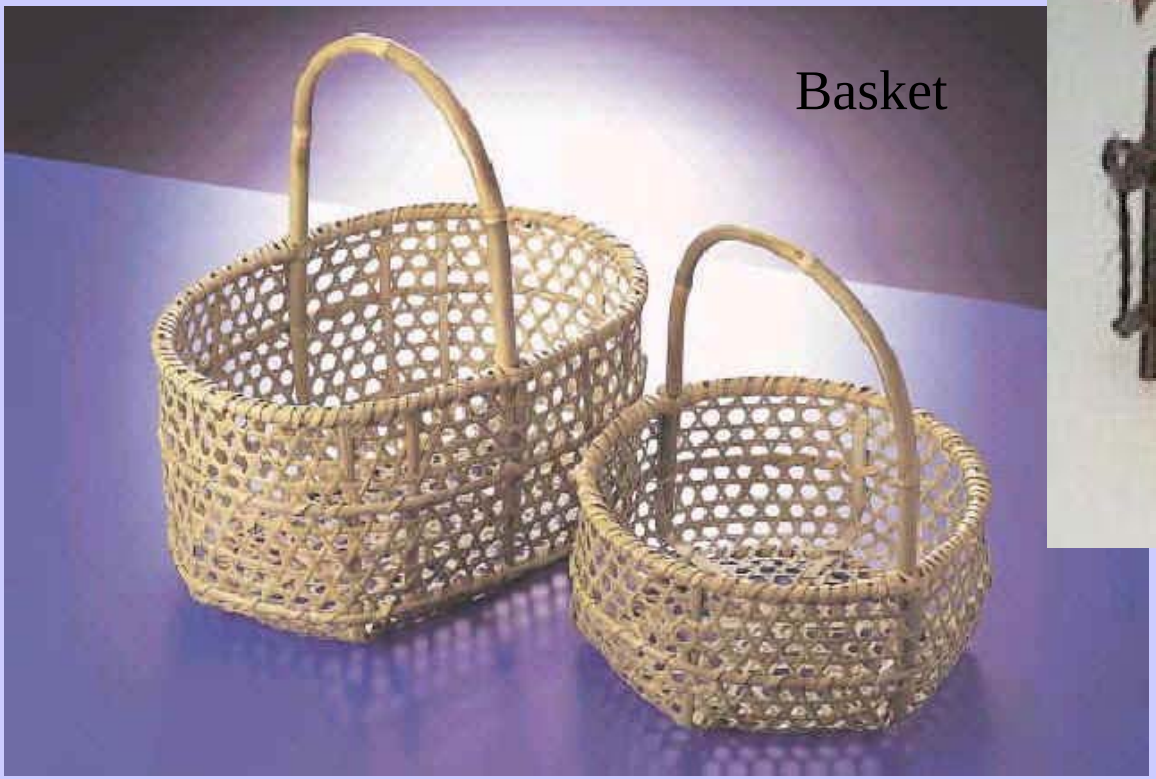

Search for Flat-band Ferromagnetism

Carbon network

Shima and Aoki, PRL **71**, 4389 (’93)
Fujita, Umeda, and Yoshida, PRB **51**, 13778 (’95)

Graphite sheet with edge (Nano graphite)

Fujita, Wakabayashi, Nakada, and Kusakabe, JPSJ **65**, 1920 (’96)
Kusakabe, Wakabayashi, Igami, Nakada, and Fujita, Mol. Cryst. Liq. Cryst. **305**, 445 (’97)

Ga or As atomic wire

Arita, Kuroki, Aoki, Yajima, Tsukada, Watanabe, Ichimaru, Onogi, and Hashizume, PRB **57**, R6854 (’98)
Yajima, Tsukada, Watanabe, Ichimura, Suwa, Onogi, and Hashizume, PRB **60**, 1456 (’99)
Okada and Oshiyama, JJAP **39**, 435 (’00)

Proposal for Flat-band Ferromagnetism in Dot Arrays

Tamura, Shiraishi, and Takayanagi, Jpn. J. Appl. Phys. **39** (2000) L241.

No clear evidence of flat-band ferromagnetism

- Synthesis or fabrication is difficult.
- Filling cannot be freely changed.
- Jahn-Teller effect usually lifts flat-band degeneracy.

Possibility of flat-band ferromagnetism in dot arrays

- Fabrication technology is well established.
- Various lattice designs are possible.
- Filling can be freely changed.
- No Jahn-Teller effect.

2D Lieb and Kagome Dot Arrays

Lieb lattice

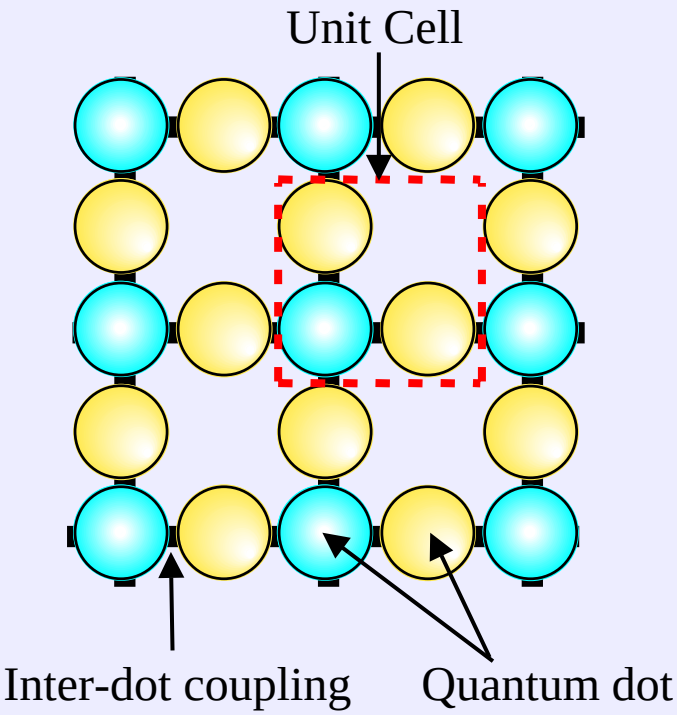

Kagome lattice

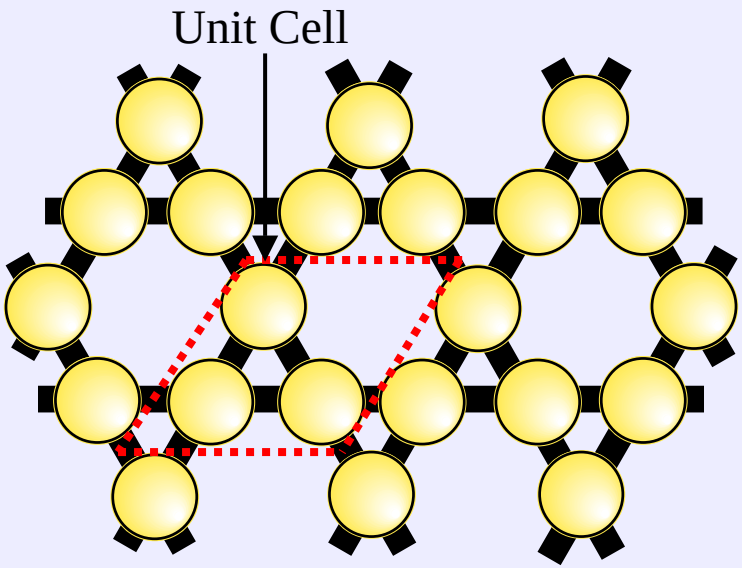

Electrons transfer between nearest-neighboring dots

Hubbard Model for Dot Arrays

Hubbard Hamiltonian

$$H = -t \sum_{(i,j),\sigma} c_{i\sigma}^{+} c_{j\sigma} + \sum_{i} U n_{i\uparrow} n_{i\downarrow}$$

(i,j) is a pair of the nearest-neighbor sites

U is the on-site Coulomb repulsion

$n_{i\sigma} = c_{i\sigma}^{+} c_{i\sigma}$

Dot model in parabolic potentials

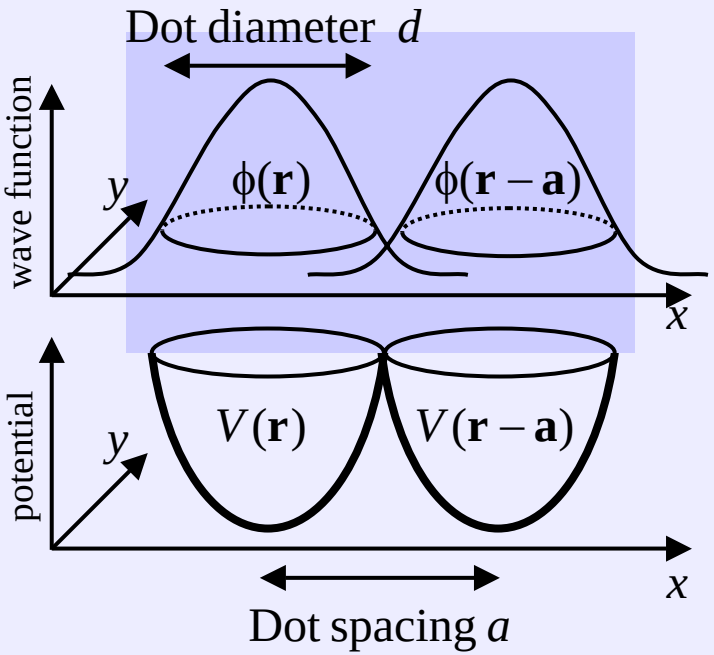

Parabolic potential

$$V(\mathbf{r}) = \frac{1}{2} m^{*} \omega^{2} \left(r^{2} - a^{2} \right)$$

Wave function

$$\phi(\mathbf{r}) = \frac{2}{\sqrt{\pi} d} e^{-\frac{2r^{2}}{d^{2}}}, \quad d \equiv 2\sqrt{\frac{\hbar}{m^{*}\omega}}$$

Transfer integral

$$t = \int d\mathbf{r}\, \phi(\mathbf{r}) \left(H_{0} + V(\mathbf{r}) \right) \phi(\mathbf{r} - \mathbf{a}) = \hbar\omega \left(1 - \frac{7a^{2}}{2d^{2}} \right) e^{-\frac{a^{2}}{d^{2}}}$$

On-site Coulomb energy

$$U = \iint d\mathbf{r}_{1} d\mathbf{r}_{2} \, \frac{\left|\phi(\mathbf{r}_{1})\right|^{2} \left|\phi(\mathbf{r}_{2})\right|^{2}}{\kappa \left|\mathbf{r}_{1} - \mathbf{r}_{2}\right|} = \frac{e^{2}}{\kappa} \frac{\sqrt{2\pi}}{d}$$

High-spin States in Lieb Lattice

Exact diagonalization of Hubbard Hamiltonian

Total spin of the GS vs. N

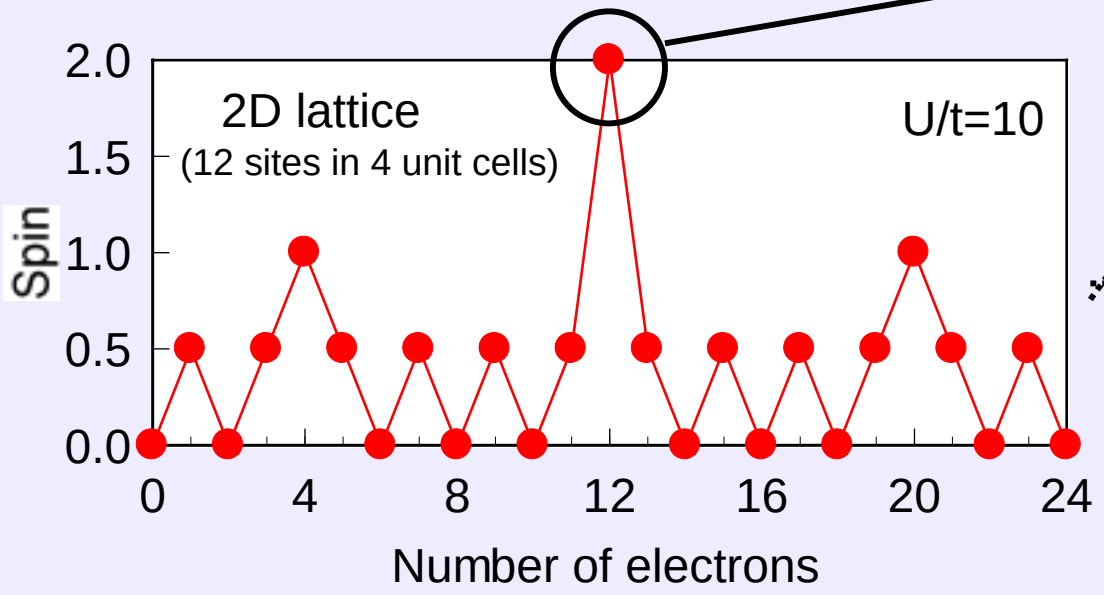

Anti-ferromagnetic ordering

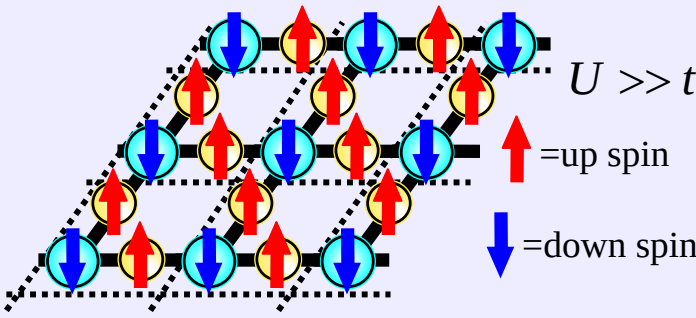

Kinetic exchange (2nd order)

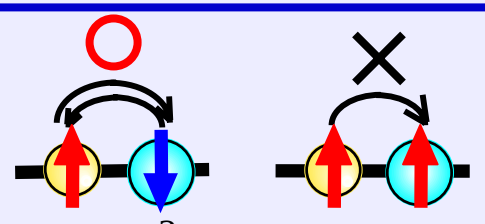

Lieb's theorem [E.H. Lieb: PRL **62** (1989) 1201]

When bands are half-filled in a bipartite lattice (one electron per site), the ground state has a spin $S=|N_A-N_B|/2$ (N_α is the number of α sites).

Stability of High Spin States

Tamura, Shiraishi, and Takayanagi, Phys. Rev. B. (2001)

Energy difference $\Delta E = E(S=0) - E(S=2)$ at half - filling

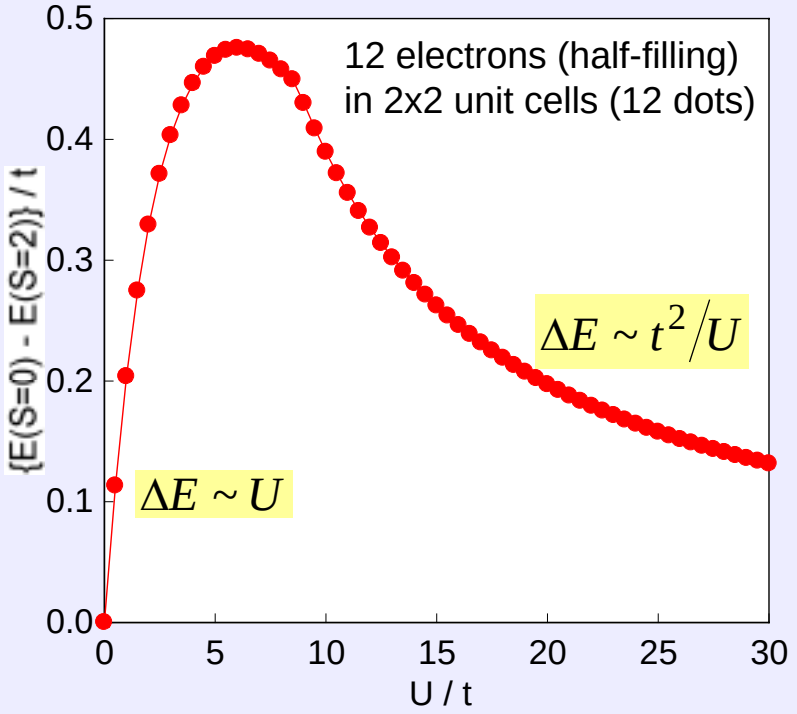

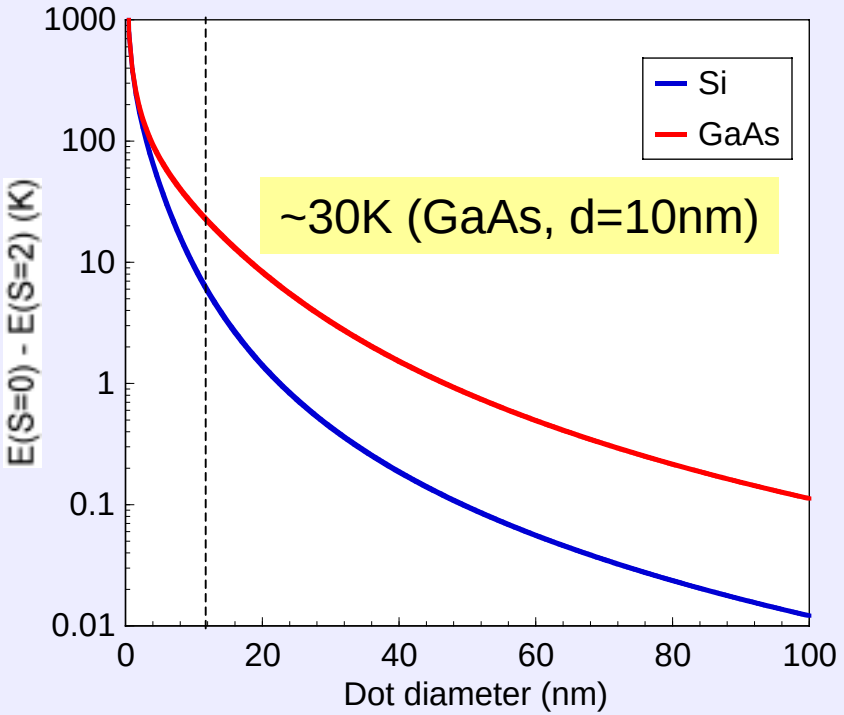

(Interdot spacing a) / (diameter d) $= 1.5$

GaAs : $m^* = 0.07, \kappa = 12$

Si : $m^* = 0.2, \kappa = 13$

High-spin States in Kagome Lattice

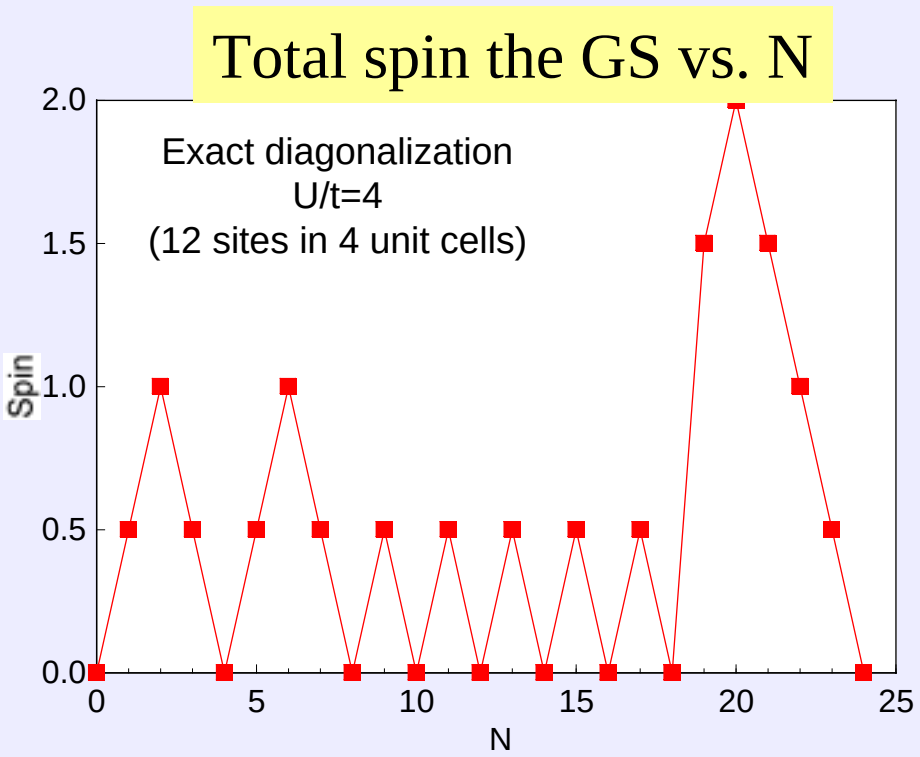

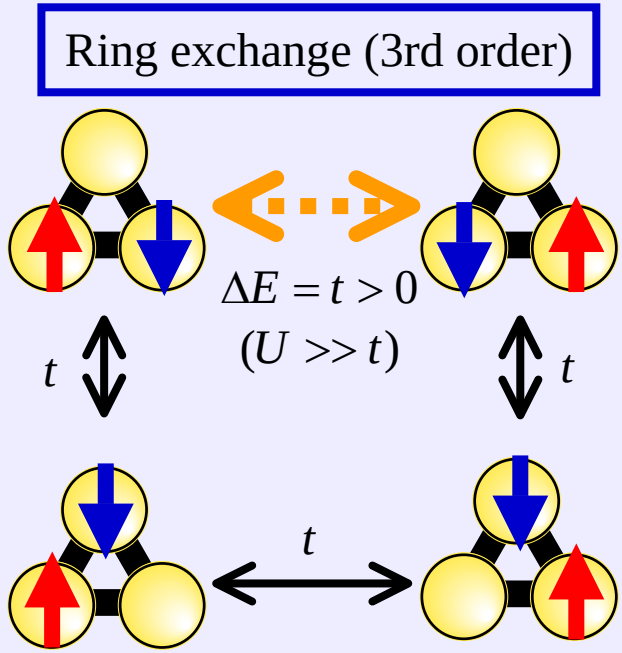

Mielke's theorem [A. Mielke: J. Phys. A**25** (1992) 4335]

Kagome lattice shows a ferromagnetic behavior for the electron filling of $5/3 < n < 11/6$.

Stability of High Spin States

Energy difference $\Delta E = E(S=0) - E(S=2)$ at $n = 5/3$ filling

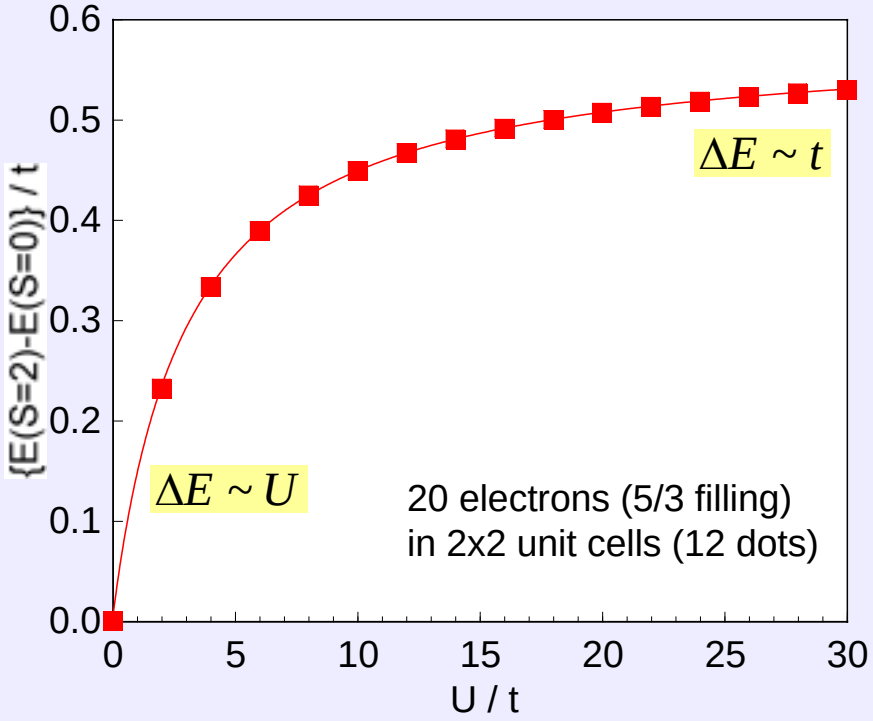

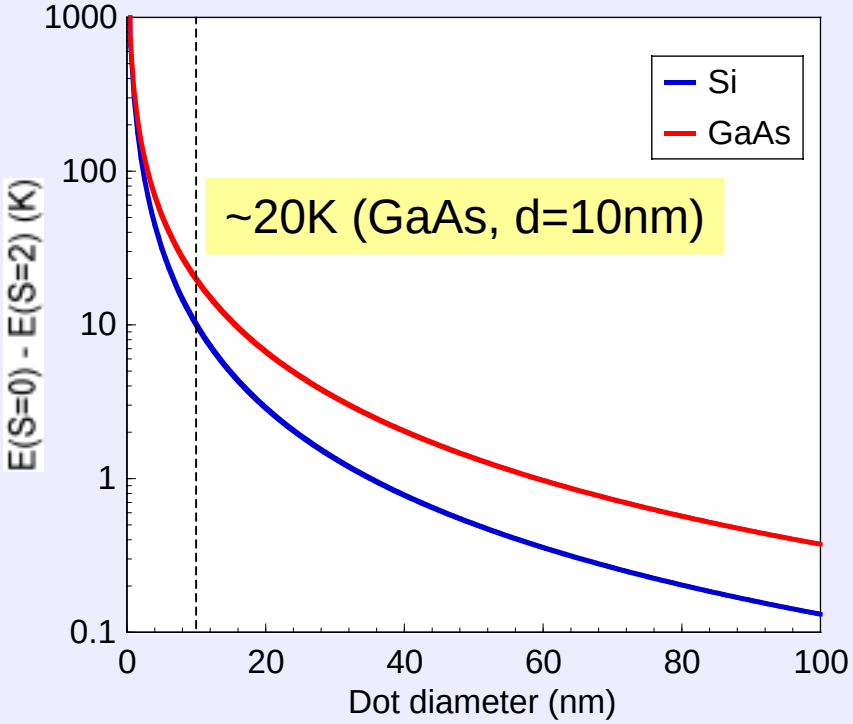

(Interdot spacing a) / (diameter d) $= 1.5$

GaAs : $m^* = 0.07$, $\kappa = 12$

Si : $m^* = 0.2$, $\kappa = 13$

Design of Kagome Solid

Kagome Network

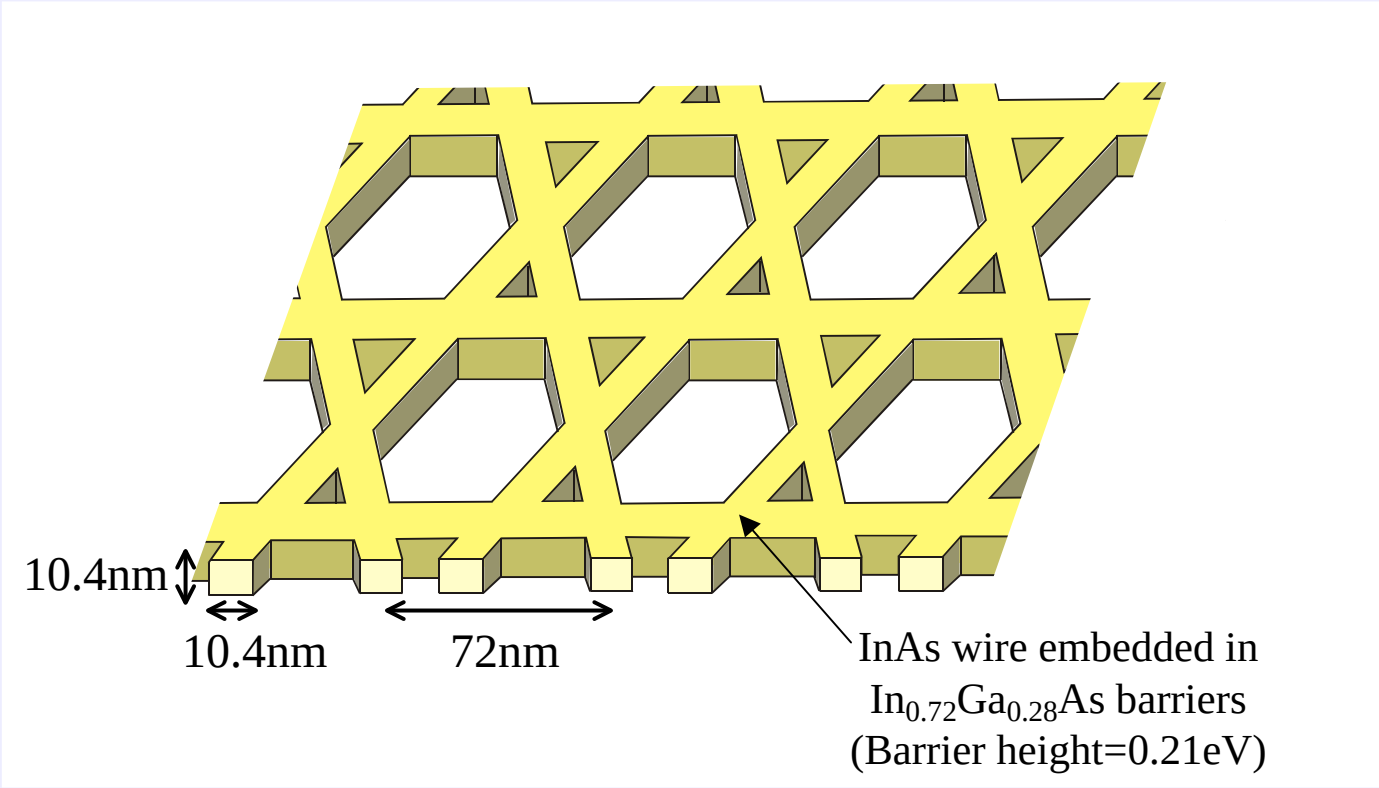

Shiraishi, Tamura, and Takayanagi, Appl. Phys. Lett. **78**, 3702 (‘01)

Band Structure of Wire Network

Band calculation by local density functional approximation

Band structure

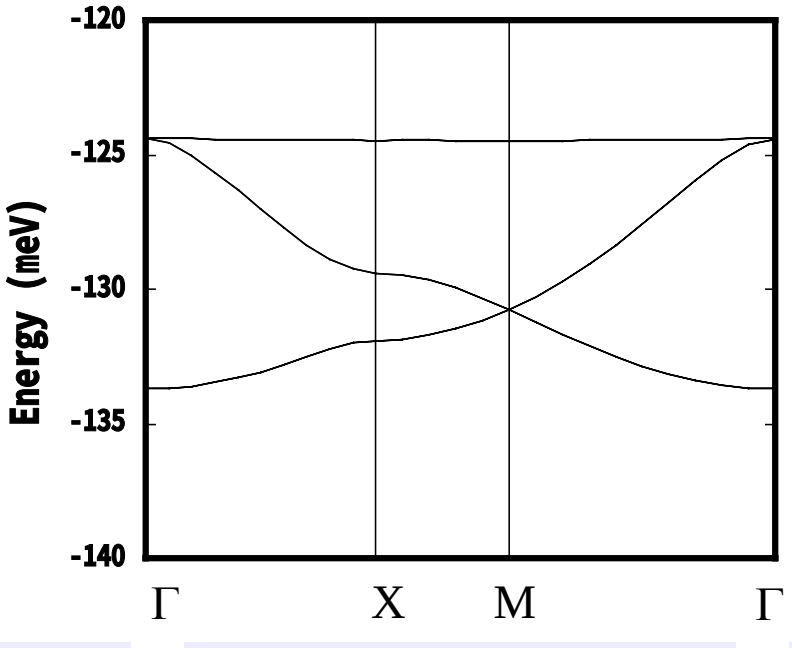

Parameter evaluation

$$\text{Band width} = 6t = 9.3\text{meV}$$

$$\downarrow$$

$$t = 1.55\,\text{meV}$$

$$\text{Hartee energy} = E_{\text{Intra-cell}} + E_{\text{Inter-cell}}$$

$$E_{\text{Intra-cell}} = N_{cell} \times n^2 \times U$$

$$(N_{cell} = 3,\ n = 5/3)$$

$$E_{\text{Inter-cell}} = (-N_{cell} ne) \times \sum_{i \neq 0}^{\text{kagome}} \frac{q_i}{r_i}$$

$$\downarrow$$

$$U = 6\,\text{meV}$$

Local spin density functional approximation

Charge distribution

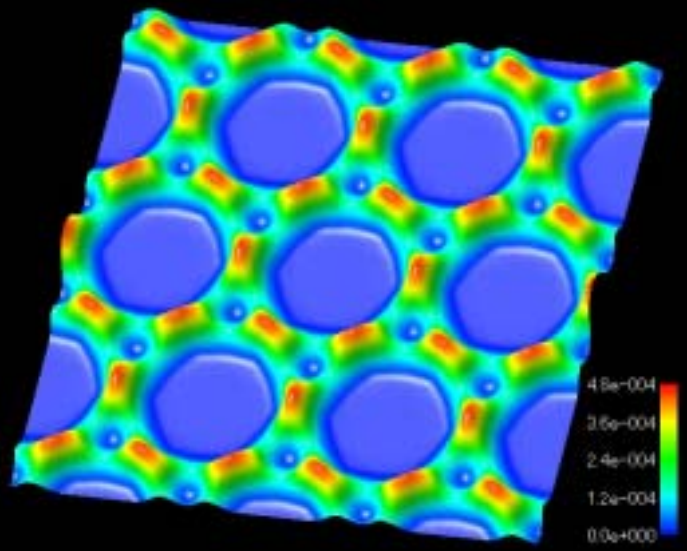

Spin distribution

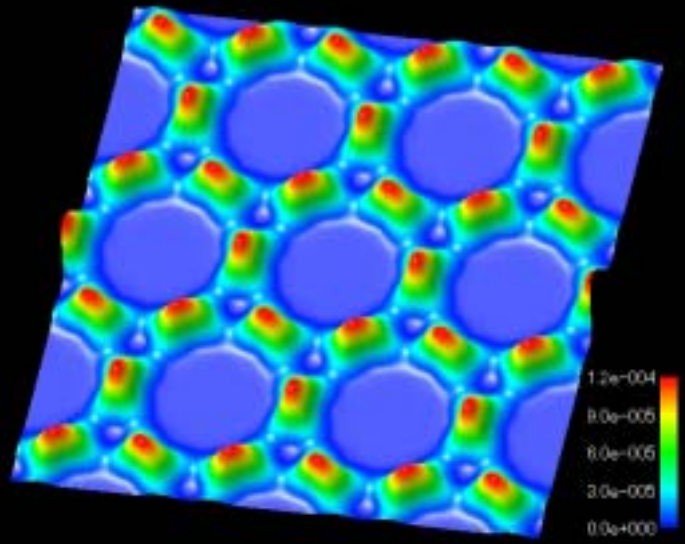

Number of electrons per dot

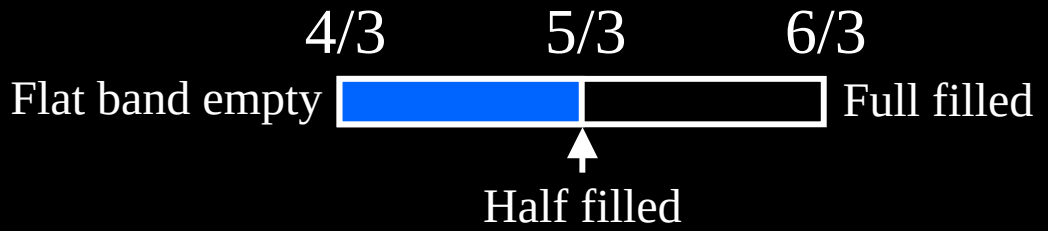

Sample Structure

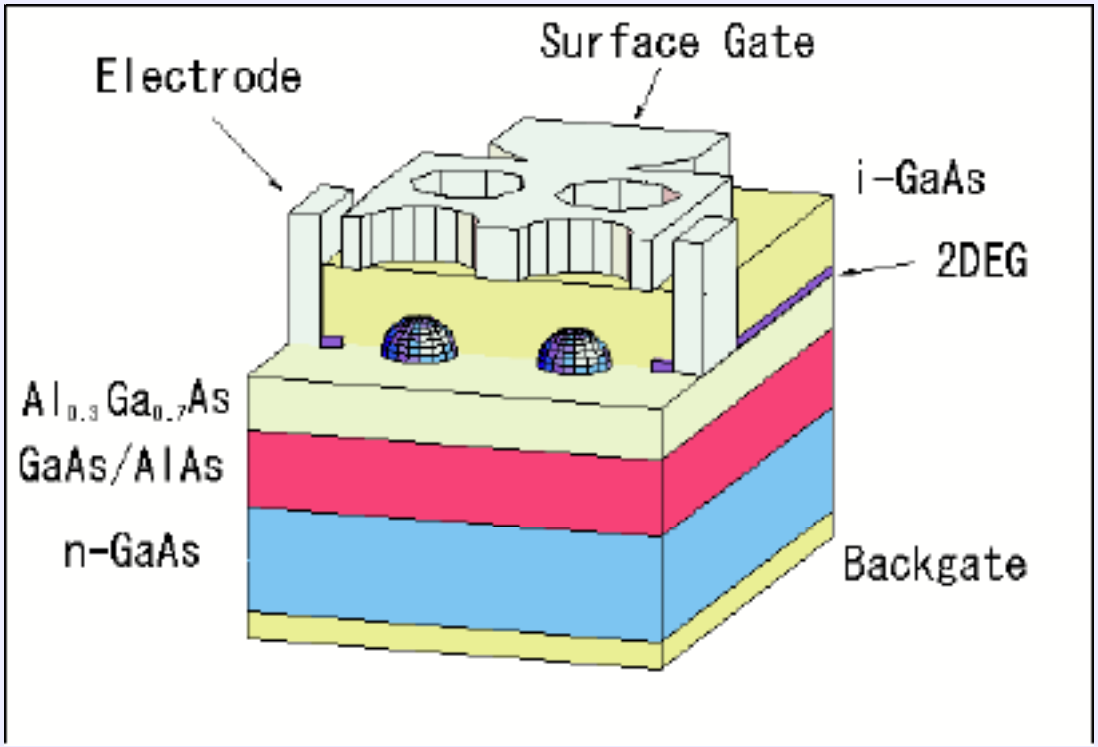

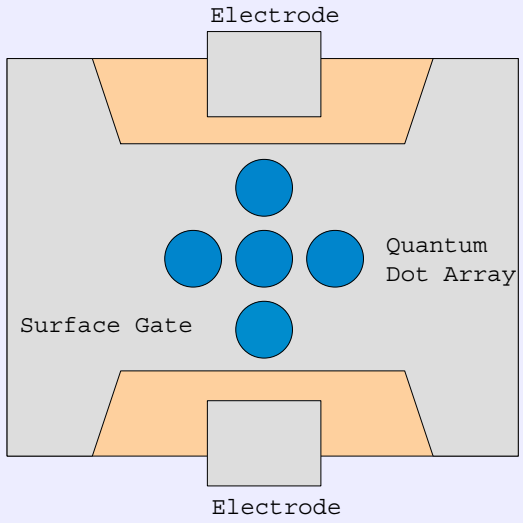

	Thickness
Ti/Au	(Surface Gate)
i-GaAs	300 nm
$Al_{0.3}Ga_{0.7}As$	20 nm
GaAs/AlAs	2.5nm/2.5nm x100
n-GaAs	(Substrate)
AuGeNi/Au	(Back Gate)

The two-dimensional electron gas (2DEG) in the heterostructure has initially no electron.
The electron density increases as the back-gate voltage increases, and finally each dot has one electron.

Undoped back-gated HEMT structure

Band structure (schematic):

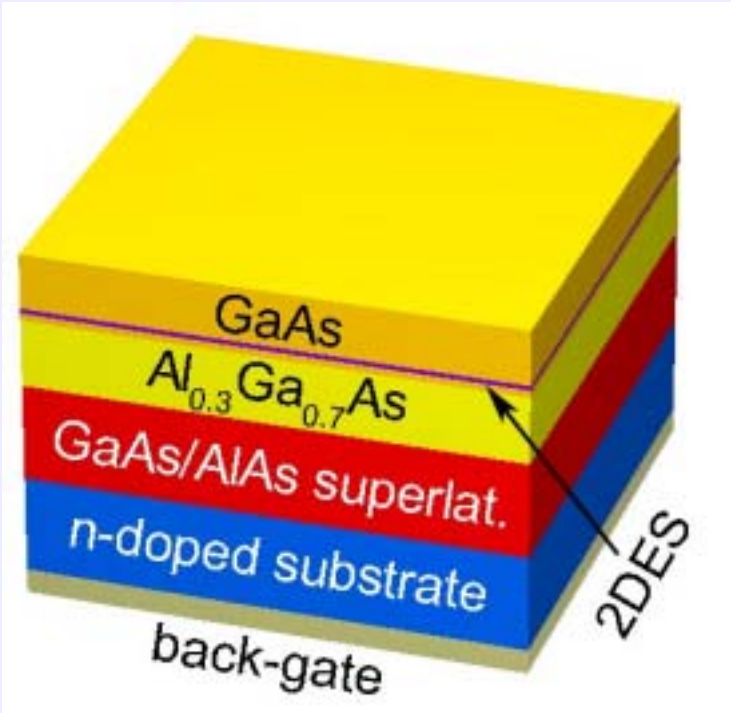

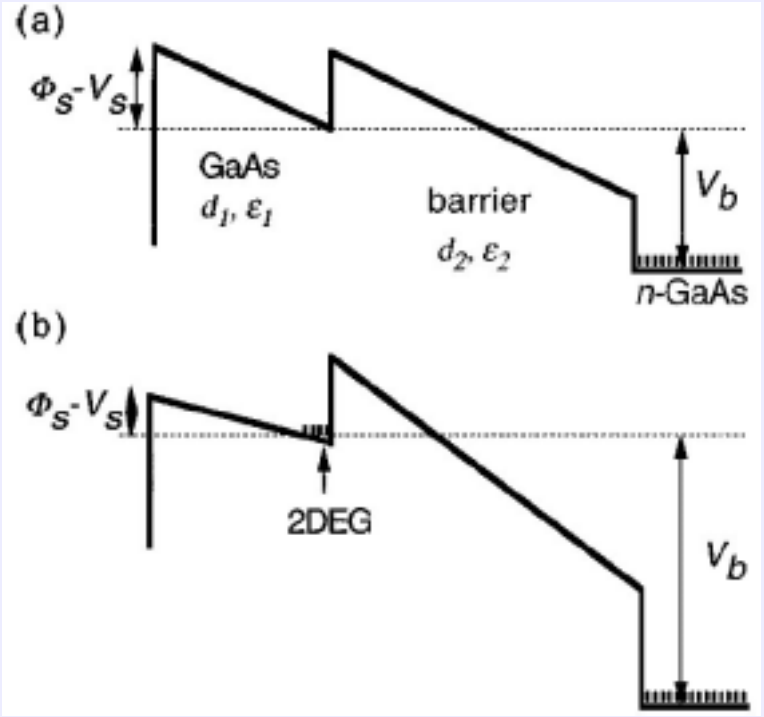

(Y. Hirayama, K. Muraki, and T. Saku, Appl. Phys. Lett. **72**, 1745 (1998))

Undoped back-gated HEMT structure

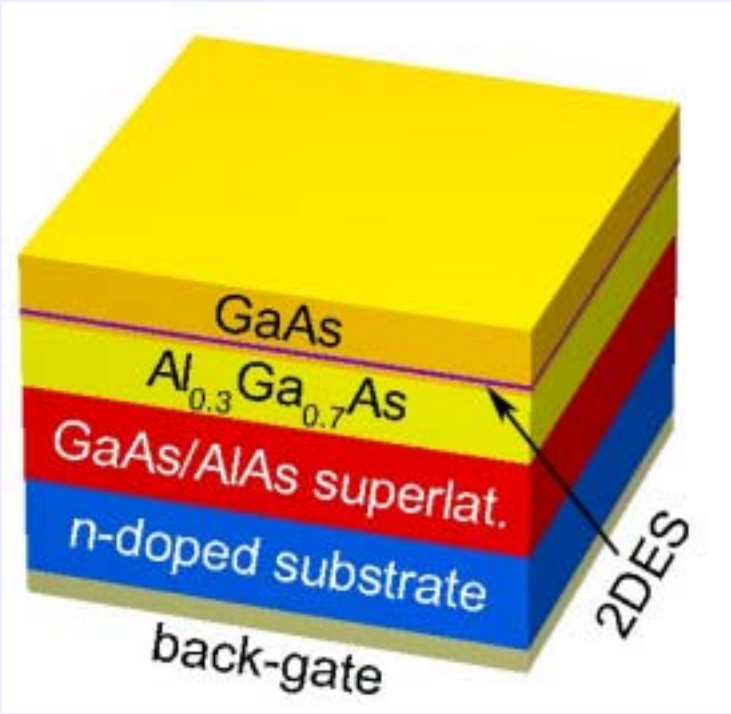

Electron density:

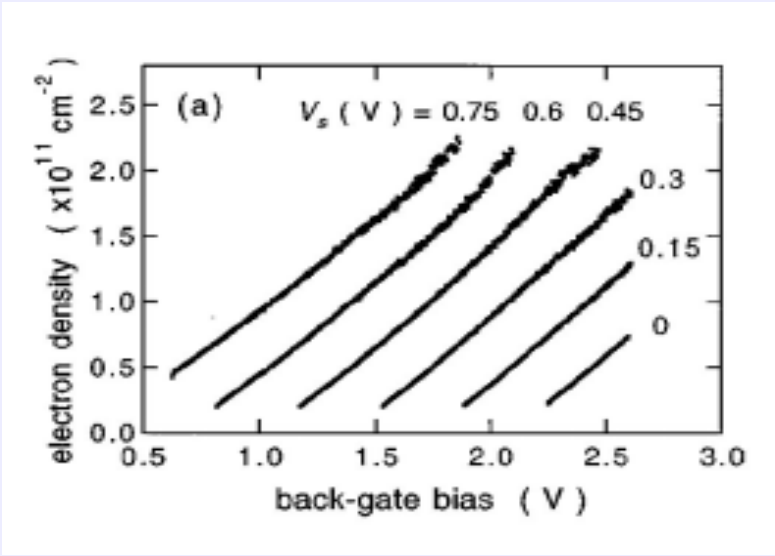

$$n = \frac{\varepsilon_1}{d_1}\left(V_{fg} - \phi_{fg}\right) + \frac{\varepsilon_1}{d_1}V_{bg}$$

Undoped back-gated HEMT structure

Electron mobility:

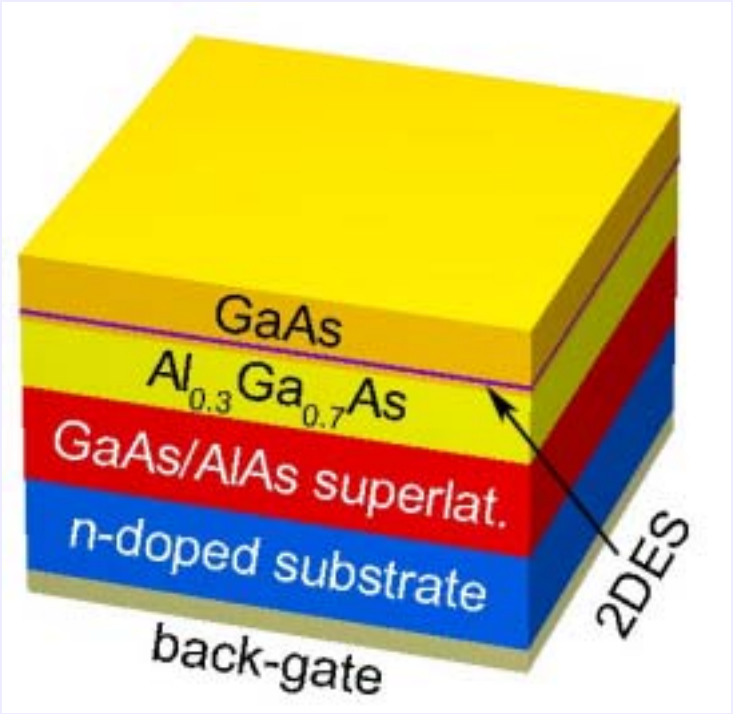

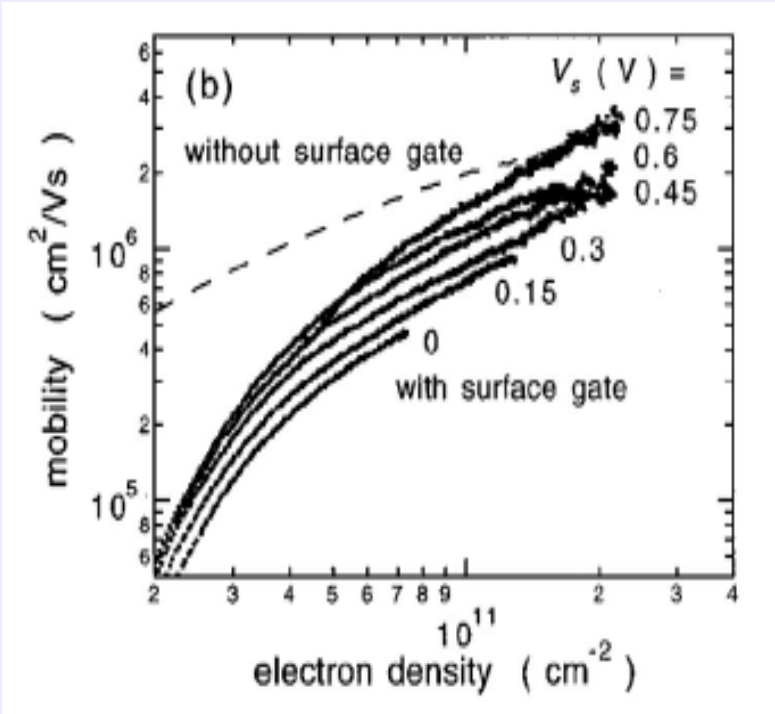

μ = 3,000,000 $cm^2V^{-1}s^{-1}$, n = $2x10^{11}$ cm^{-2} -> l_{el} = 22 μm

μ = 200,000 $cm^2V^{-1}s^{-1}$, n = $3x10^{10}$ cm^{-2} -> l_{el} = 570 nm

Quantum dot with a single front-gate

Scanning electron micrograph

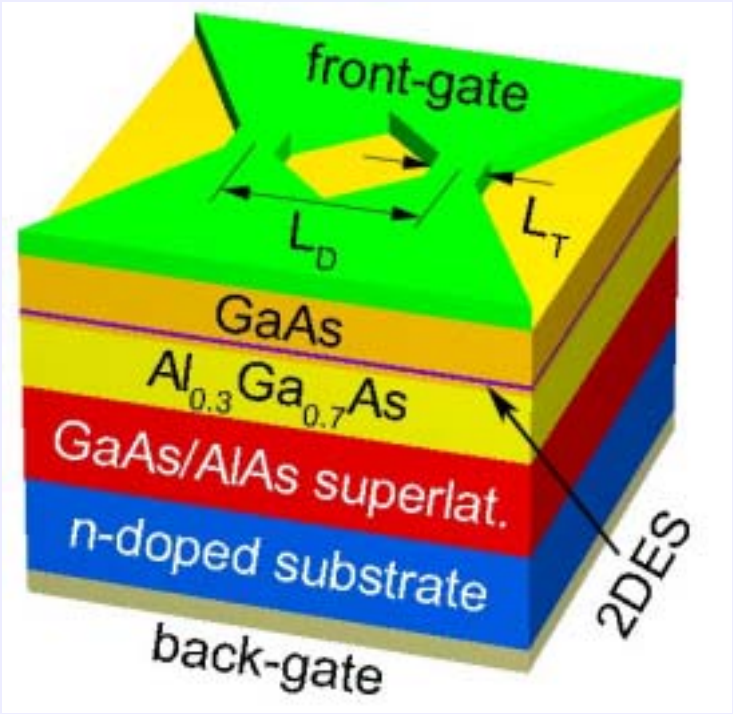

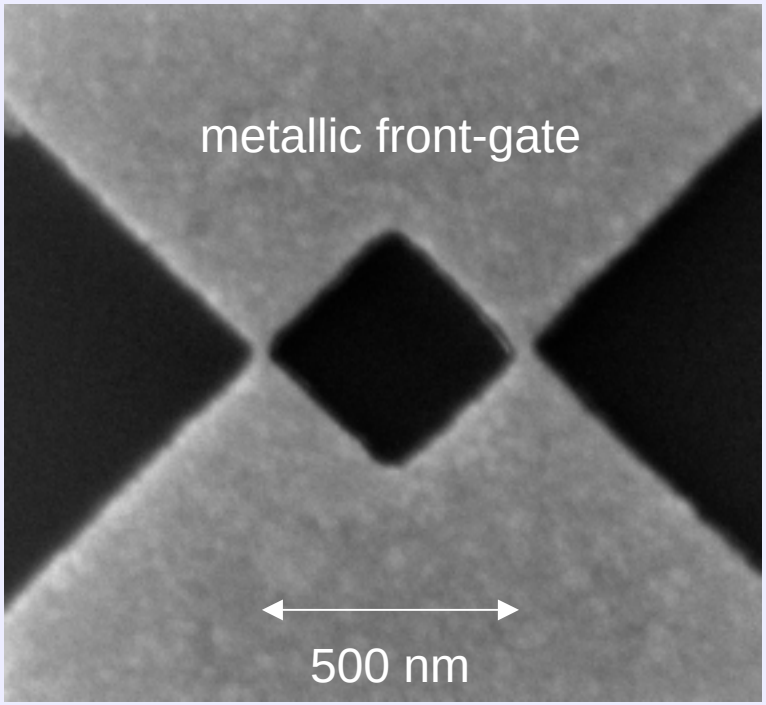

Single quantum dot – front-gate dependence

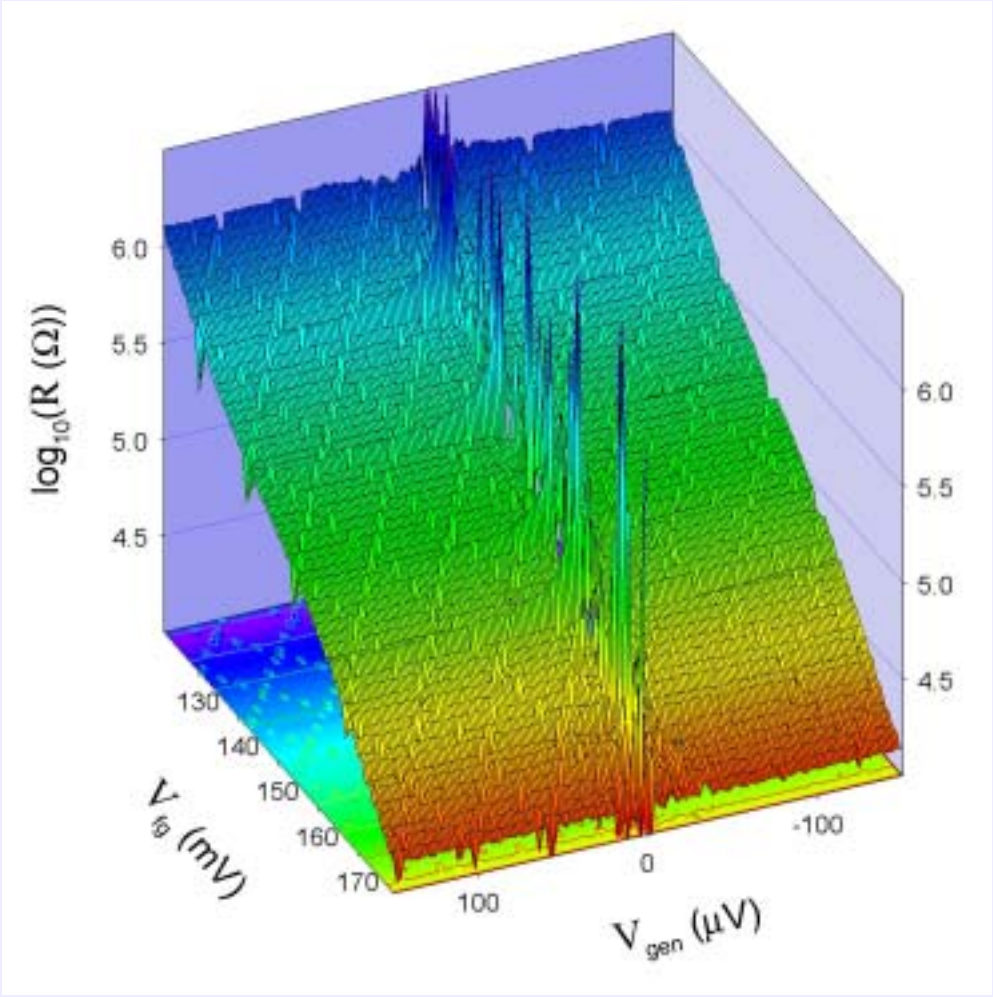

- Nice Coulomb diamond structure !
- Peaks at low bias related to DC measurement proc.
- Sample resistance changes by two orders of magnitude -> V_{sd} changes

Single quantum dot – peak positions

Peak positions:

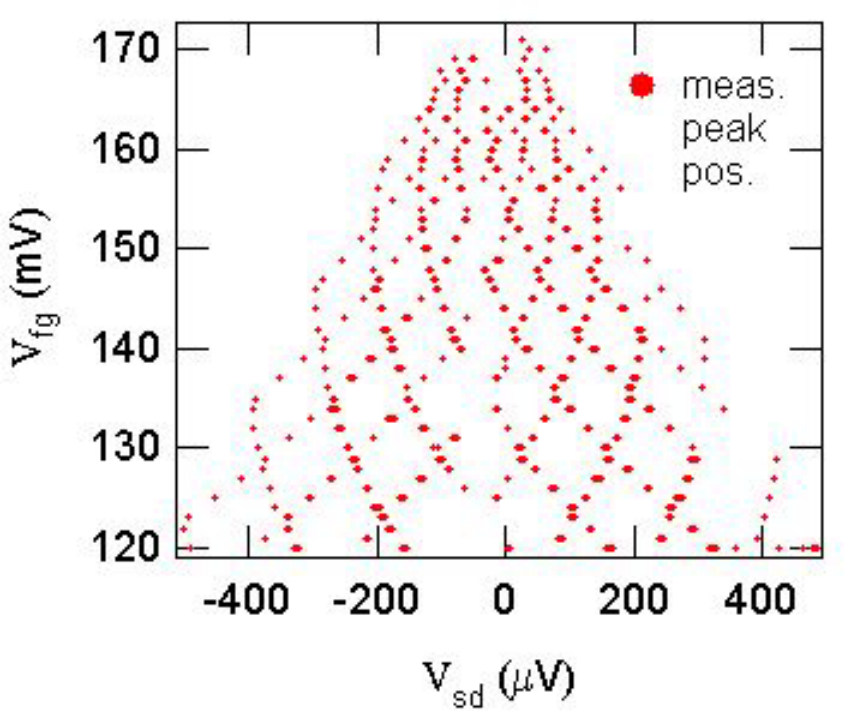

Single quantum dot – simulations

Peak positions:

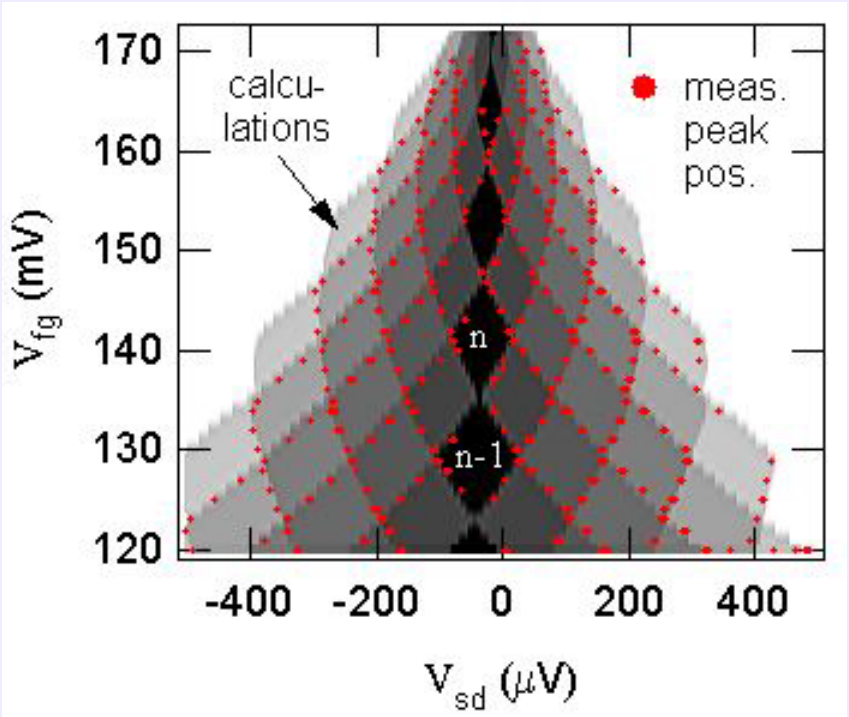

Total and gate-capacitance:

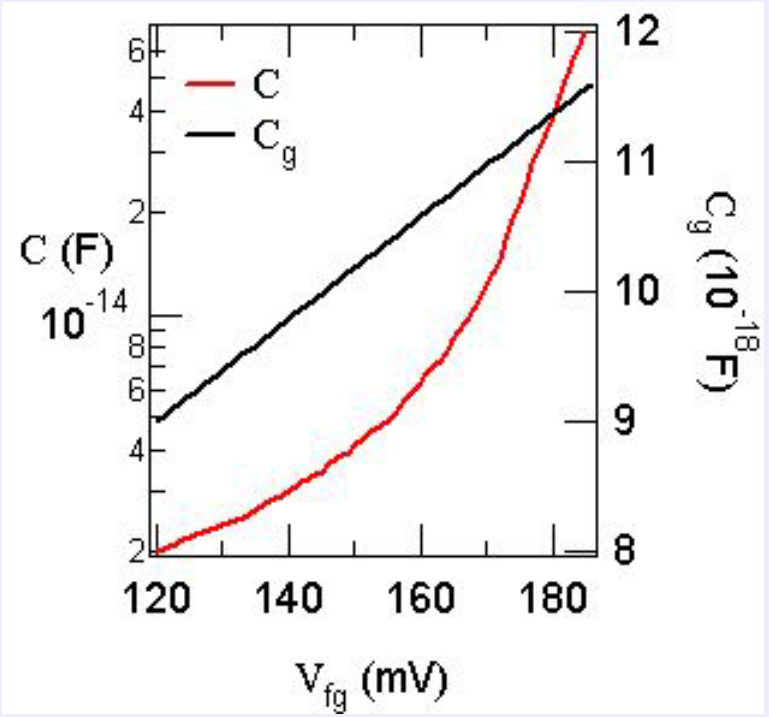

Front-gate has threefold impact:

(a) shift dot spectrum, (b) change tunnel barriers, (c) change dot size

Quantum dot arrays

Kagome lattice:

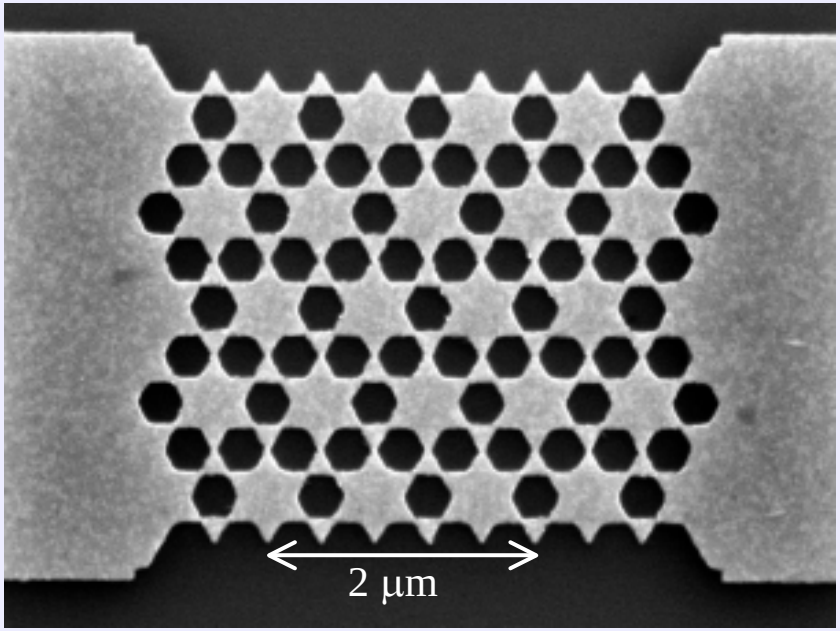

Rhombic lattice:

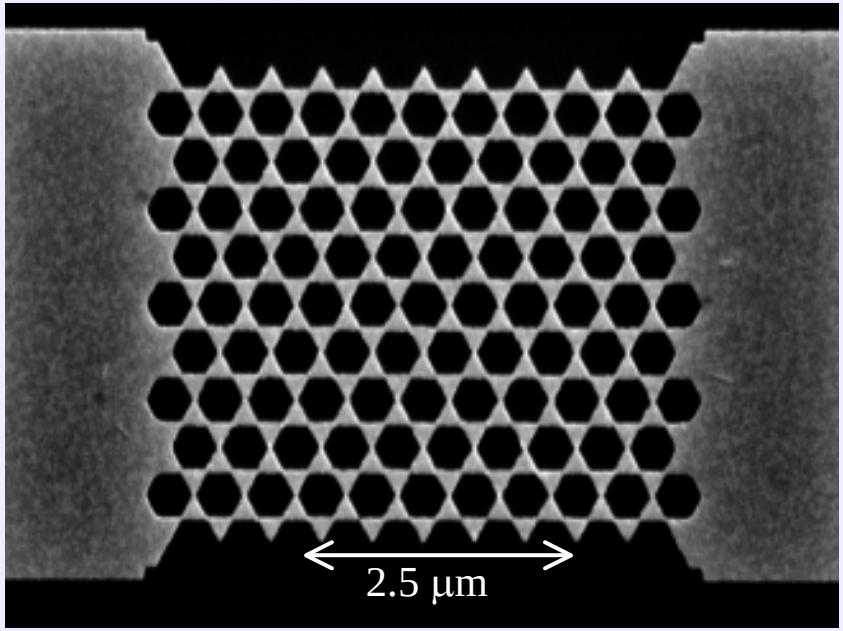

Superconductivity with electronic mechanism

Kimura et.al., (2002)

Conventional BCS superconductors

↕

High-T_c superconductors

d-wave superconducting paring

Antiferromagnetic phase near the superconducting phase suggesting a strong antiferromagnetic fluctuation

Anomalous metal phase:
transport or magnetic properties, spin gap, etc…

↓

ossibility of electronic mechanism for superconductivity.

owever, the phonon mechanism is not completely neglected.

↕

In quantum-dot superlattices, we can study superconductivity with electronic mechanism and with negligible phonon.

Phase diagram of High-T_c cuprat

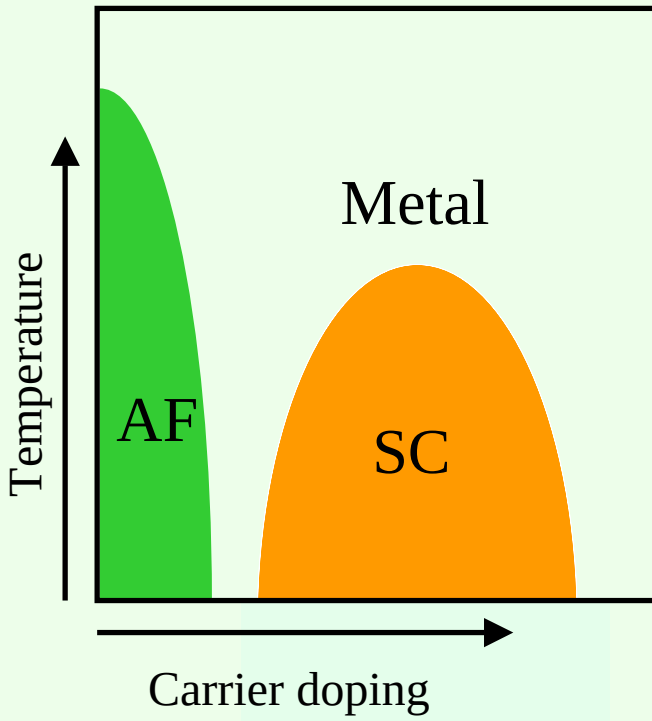

Superconductivity of the Hubbard model

The Hubbard model is a possible relevant model for cuprates, including the interaction between electrons with opposite spins on lattice points.

A virtual process of the Hubbard model near/at the half-filling

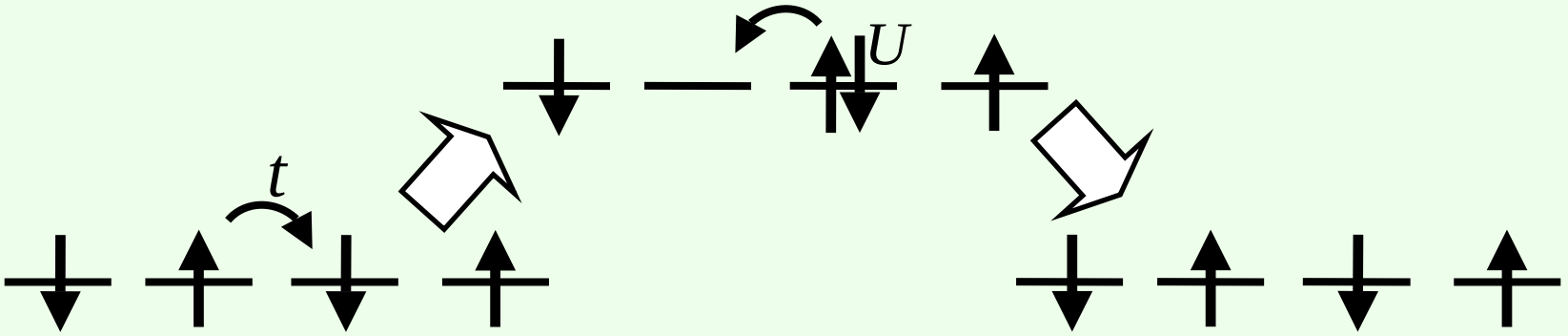

Effective antiferromagnetic coupling between adjacent spins $\approx 4t^2/U$

We employ the fluctuation-exchange (FLEX) approximation (a self-consistent RPA). FLEX is an excellent tool to treat a strong antiferromagnetic spin-fluctuation and gives a reliable T_c (about 100K for cuprates).

Bickers et al., PRL **62**, 961 (1989).

Our lattice design with a quantum wire network

InAs wires embedded in $In_{0.776}Ga_{0.224}As$ with the barrier height=0.17eV

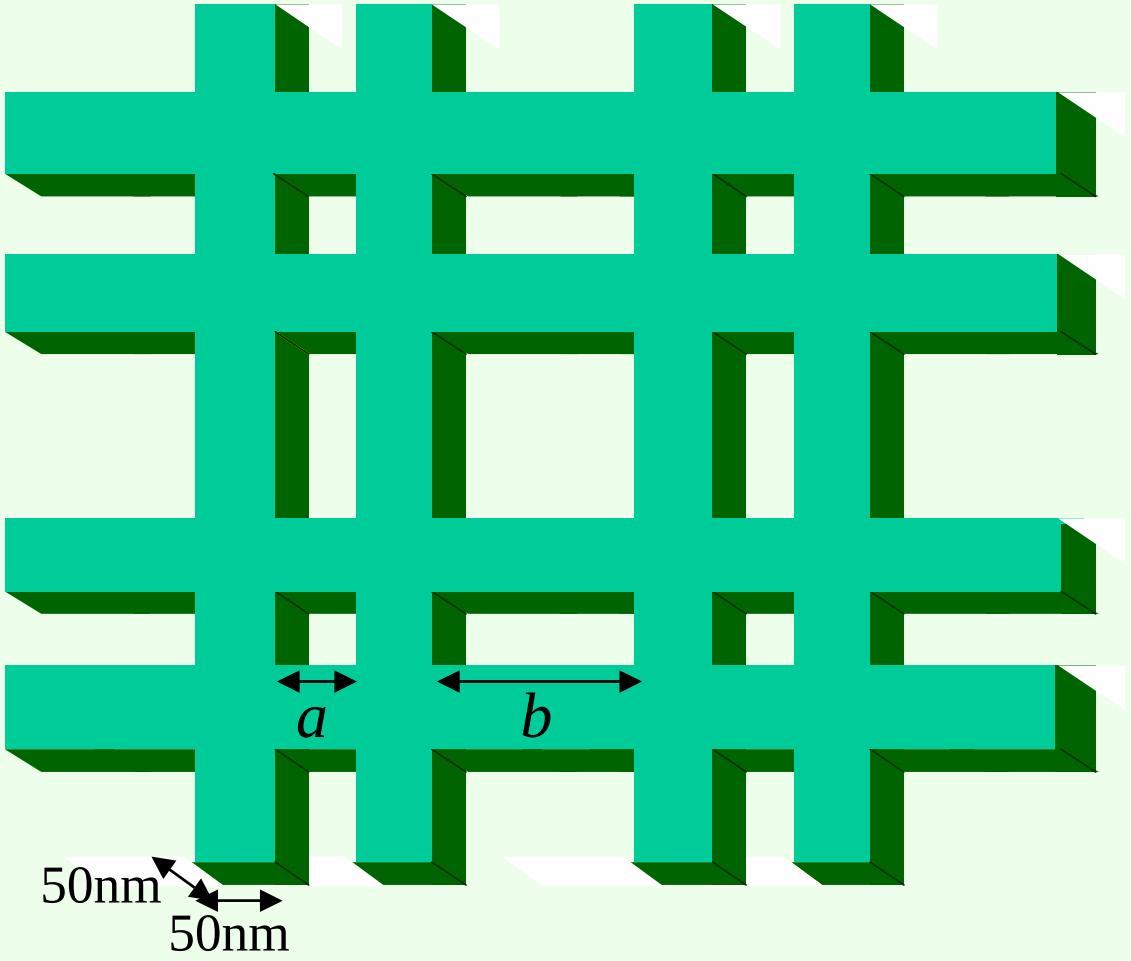

$a=b$=61.1nm for a square lattice

a=38.8nm and b=83.4nm for a plaquette lattice

The Hubbard model on a plaquette lattice

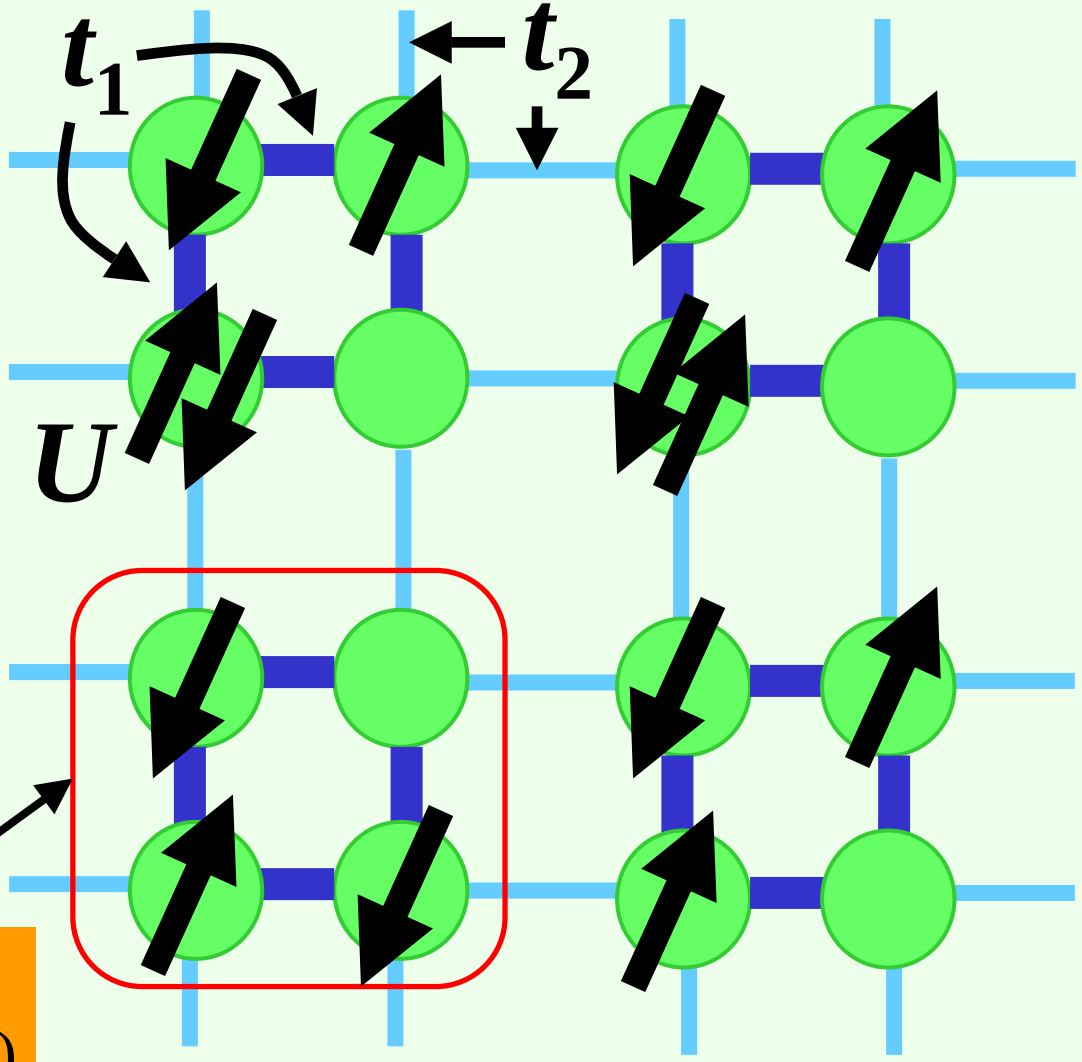

Unit cell
(plaquette)

A square lattice is reproduced at $t_1 = t_2$.

Lattice structure dependence of T_c

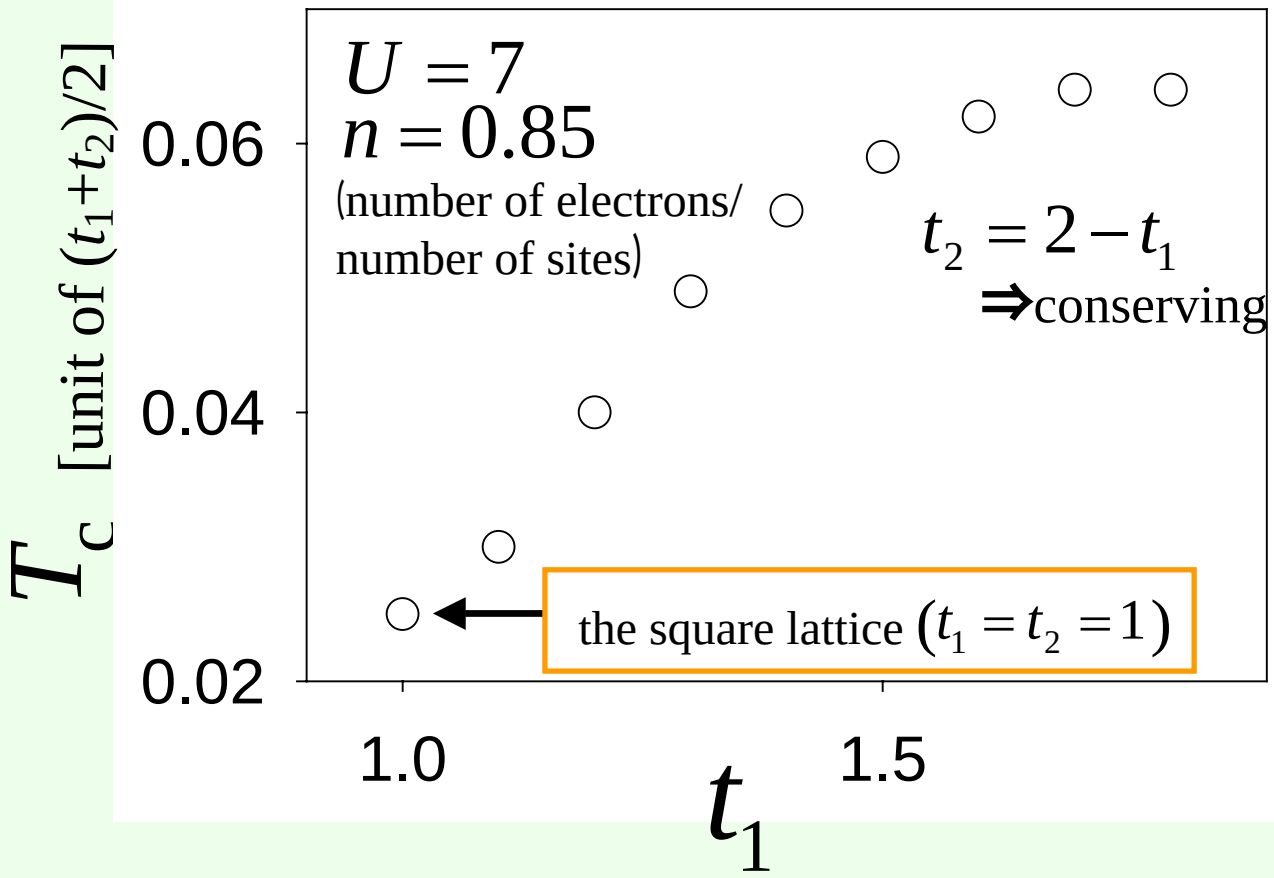

For our design with an InAs wire network:

$T_c \approx 40$ mK for a square lattice.

$T_c \approx 90$ mK for a plaquette lattice.

How is T_c of the Hubbard model decided?

1. A self-consistent calculation with FLEX approximation

⟶ The Green's function $G(\vec{k})$ and the antiferromagnetic spin susceptibility $\chi(\vec{k})$

2. Solving the Eliashberg's equation

⟶ Determination of T_c and the superconducting gap function $\phi(\vec{k})$

The Eliashberg's equation

$$\phi(\vec{k}) = -\sum_{\vec{k}} \frac{V_{\text{eff}}(\vec{k}-\vec{k}')}{2\xi(\vec{k})} \tanh\left(\frac{\xi(\vec{k})}{2k_B T}\right)\phi(\vec{k}')$$

$$V_{\text{eff}} \approx -\frac{\langle \chi(\vec{k}-\vec{k}')\phi(\vec{k})\phi(\vec{k}')\rangle}{\langle \phi(\vec{k})^2 \rangle}$$

$\langle \cdots \rangle$: average over Fermi surfaces

Generally speaking, we obtain a larger T_c for larger V_{eff}.

Why is T_c of the plaquette lattice enhanced?

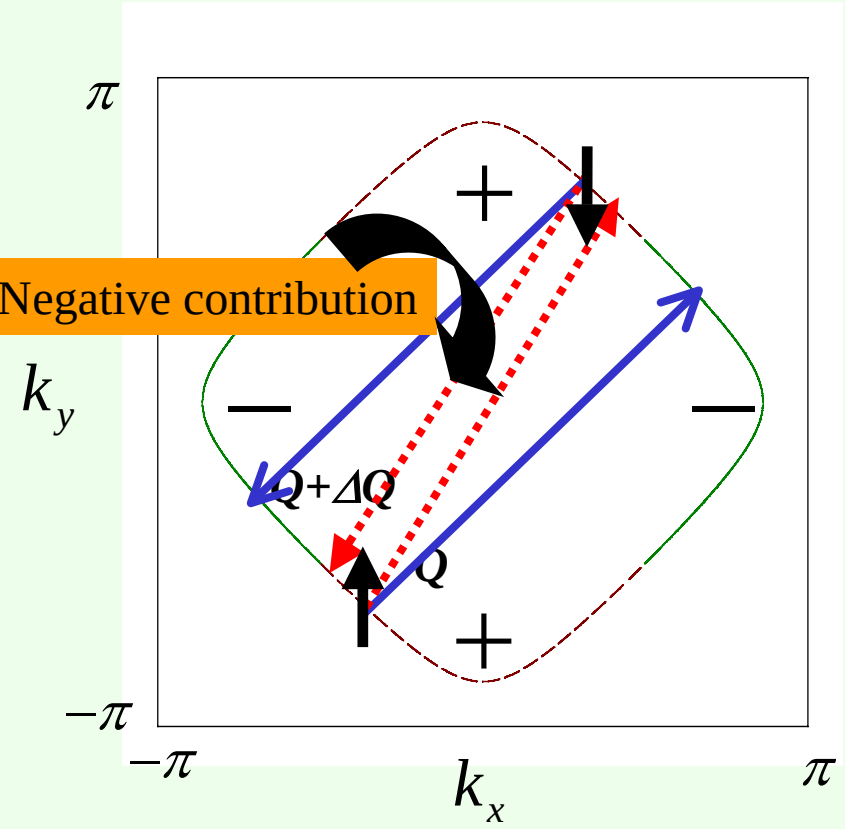

Negative contribution

Square lattice

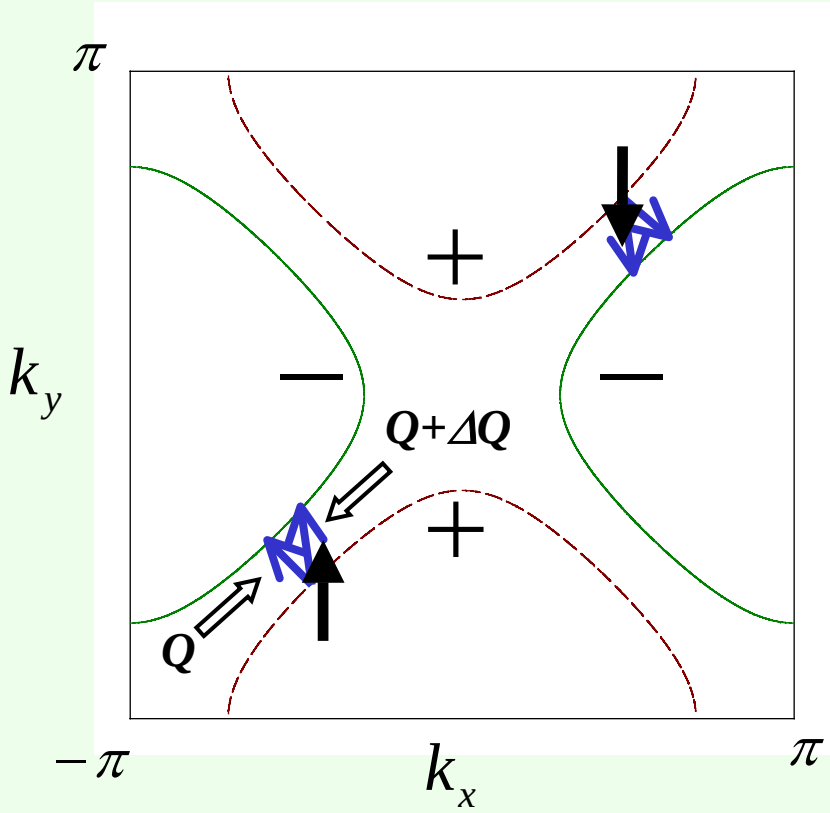

Plaquette lattice

A Pair scattering (Red dashed lines) connects points where the gap functions have the same sign, resulting in a negative contribution to superconductivity.

Because of disconnected Fermi surfaces, pair-scatterings with negative contribution to superconductivity are absent.
→ a very high-T_c

Disconnected Fermi surfaces ⇒ a high T_c [Kuroki&Arita, PRB 64, 024501 (2001)]

Green function

(a)

$|G|^2$

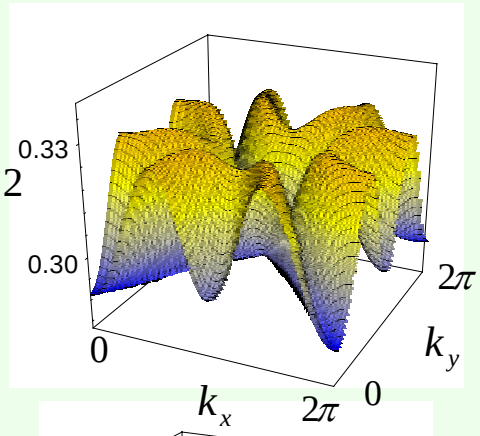

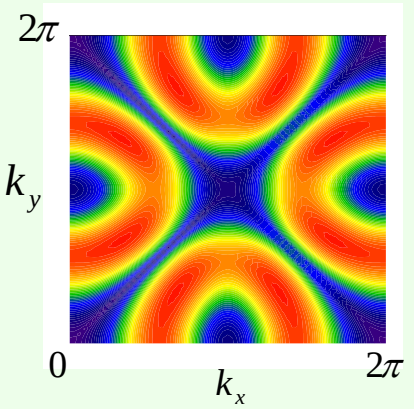

Spin susceptibility

(b)

χ

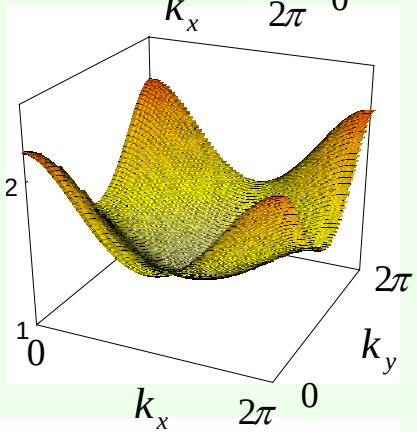

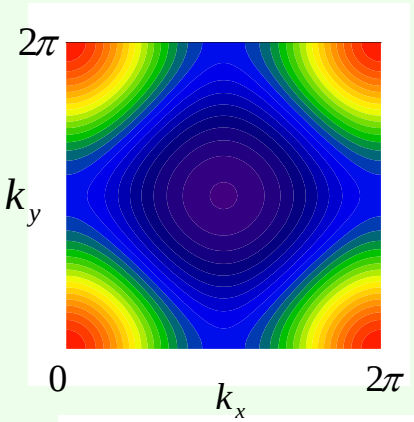

Gap function

(c)

ϕ

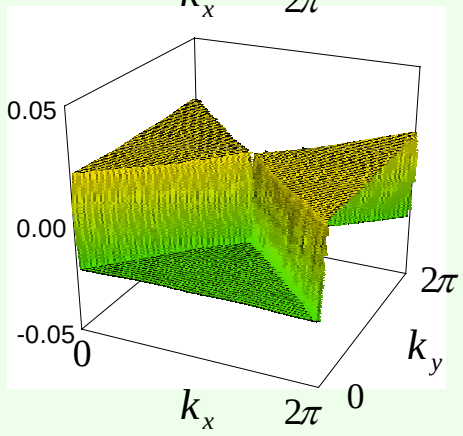

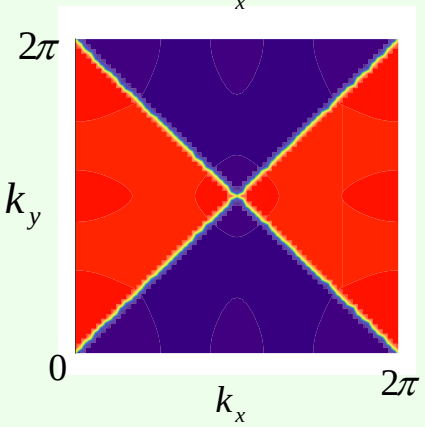

Summary

- Material design using semiconductor dot arrays is proposed.
- Flat-band ferromagnetism in dot arrays is discussed.
- Advantages of using semiconducting materials for dot-array ferromagnets are pointed out.
- Superconductivity using dot arrays are proposed.